Ammoxidation of α-Methylstyrene to Atroponitrile over U–Sb–Oxide Catalysts

ROBERT K. GRASSELLI, JAMES D. BURRINGTON, DEV D. SURESH,
MARIA S. FRIEDRICH, AND MARY ANN S. HAZLE

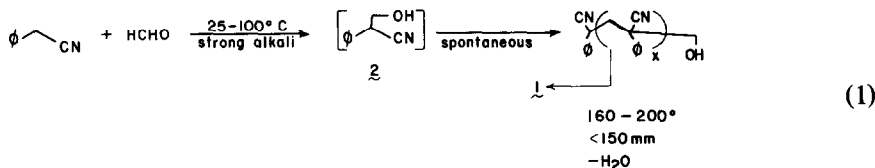*Department of Research and Development, The Standard Oil Company (Ohio), 4440 Warrensville Center Road, Warrensville Heights, Ohio 44128*

Atroponitrile (α-phenylacrylonitrile) can be synthesized by the direct catalytic ammoxidation of α-methylstyrene. Conversions to atroponitrile of 57% per pass with a selectivity of 85% are attained using a Nb-promoted $USb_{4.6}O_{13.2}$ catalyst. Several other U–Sb–oxide catalysts give similar results. A detailed study of reaction variables shows that an optimal yield of atroponitrile is formed under conditions of short contact times (0.5 sec), low surface area (7 m²/g), low feed: air + diluent ratio (1/120), and N_2 dilution. The structure of the major product of α-methylstyrene ammoxidation has been unambiguously determined as α-phenylacrylonitrile by ir, NMR, and low-voltage mass spectrometry. Atroponitrile dimerizes to 1,4-dicyano-1-phenyl-1,2,3,4-tetrahydronaphthalene (DPT) in benzene solution with second-order kinetics and an E_a of 14.8 kcal/mole, typical of other Diels–Alder reactions. The dimer exists in both crystalline and amorphous forms. The rate of cinnamonitrile formation from ammoxidation of allylbenzene is 2.9 times faster than from β-methylstyrene, suggesting that the ammoxidation of aromatic olefins proceeds through a common allylic intermediate.

INTRODUCTION

Atroponitrile (α-phenylacrylonitrile) (1) possesses the potential as both a valuable polymer building block, and a reactive synthetic intermediate (1–7). The synthesis of atroponitrile to date consists of several techniques, including two patented processes, both of which are expensive, cumbersome, and strictly limited to laboratory scale.
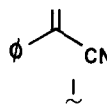
In the first of these, phenylacetonitrile is condensed with formaldehyde in the presence of strong alkali to form hydrated atroponitrile intermediate (2) which spontaneously self-condenses to form a dimer, trimer, and polymer mixture (molecular weight 225–375), which is then flash vaporized to form atroponitrile (8) (Eq. (1)).

$$ \phi \diagdown_{CN} + HCHO \xrightarrow[\text{strong alkali}]{25-100^\circ C} \left[\phi \diagdown \begin{smallmatrix} OH \\ CN \end{smallmatrix} \right] \xrightarrow{\text{spontaneous}} \begin{smallmatrix} CN \\ \phi \end{smallmatrix} \begin{smallmatrix} CN \\ \phi \end{smallmatrix}_x OH $$

$$ \underset{\substack{160-200^\circ \\ <150 mm \\ -H_2O}}{\xrightarrow{}} 1 \tag{1} $$
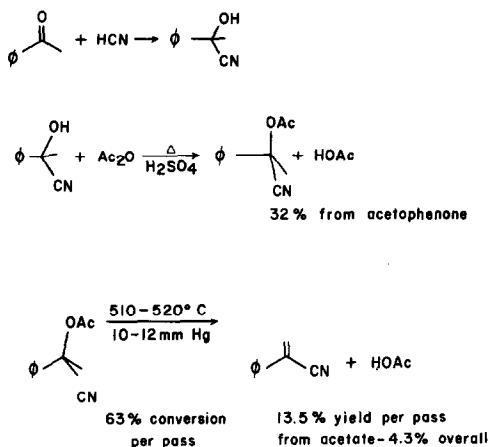
While yields of up to 90% can be achieved by the process, the duration of the reaction (several hours), the cost of starting materials, and the rigorous controls of temperature and pressure on the reaction and flash pyrolysis steps, necessary to avoid polymerization, render it economically unattractive for industrial application. It does,

however, appear to be the most widely used laboratory preparation of atroponitrile (5, 6, 9, 10).

The second process is described in this 3-step reaction sequence (11).

32% from acetophenone

63% conversion per pass   13.5% yield per pass from acetate—4.3% overall

This process is even more cumbersome than the previous route. It requires three steps, cyanoethylation of acetophenone to acetophenone cyanohydrin, the acetylation of the cyanohydrin, and the pyrolysis of the resulting cyanohydrin acetate, all of which need good reaction control. This fact, coupled with the low yields, renders this process of no practical value.

An array of copolymers of atroponitrile have been reported, including those derived from butadiene (1), carboxylic butadiene derivatives (1), chlorinated vinylidene derivatives (1), ethylene (2), and styrene derivatives (2). Polymeric atroponitrile has also been reported (3). Although the properties of these copolymers are not discussed, it is expected that they may be superior to ABS resins because of anticipated higher crystallinities. The expected polymerization of atroponitrile to give a carbon chain with each alternating carbon having both a phenyl and a nitrile group should result in a homopolymer of higher order of regularity than a styrene-acrylonitrile copolymer of the same empirical composition (i.e., a 50/50 composition, in which block polymerization of the type

—S–S–S–A–A–S–A–A is virtually unavoidable). The intramolecular repulsion forces in atroponitrile homopolymer are expected to result in a stereoregular helical arrangement, i.e., a syndyotactic polymer. Such highly stereoregular polymers are generally desirable because they usually possess high temperature resistance, high impact strength, and high flexibility.

Other useful reactions of atroponitrile include its spontaneous dimerization at room temperature to form 1,4-dicyano-1-phenyl-1,2,3,4-tetrahydronaphthalene (4, 5). A variety of dibasic acids, diamines, diamides (4, 5), and diguanamine (20) derivatives have been prepared from the dimer and are expected to be used in polyester and polyimid resins if atroponitrile can be made economically on a large scale. In addition, atroponitrile undergoes a variety of rapid reactions as a Michael acceptor with a number of nucleophiles including amines, thiols, and alkoxides (5, 6, 22), and active methylene compounds such as ketones, esters, nitriles, 1,3-dicarbonyl compounds, and α-cyanoesters (3, 4, 7) to form useful synthetic intermediates.

In light of the potential utility of atroponitrile, we have explored the catalytic ammoxidation of α-methylstyrene (12, 13, 19) as a more direct route to large-scale production of atroponitrile.

The key to the successful direct ammoxidation of α-methylstyrene to atroponitrile (Eq. (2)) lies in the tailoring of

$$(2)$$
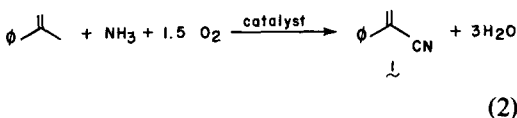
the catalyst properties so that the ammoxidative attack will occur on the methyl group of α-methylstyrene without elimination of the methyl and methylene groups from the molecule. The initial attack has to occur by an abstraction of a methyl hydrogen and the formation of an allylic intermediate 3.

The intermediate which is complexed to the catalyst site is then further attacked by activated nitrogen ($-NH$) on either of the two terminal carbon atoms. The product atroponitrile is desorbed, and the surface site, which is depleted of active oxygens, i.e., reduced during the course of the reaction, is reoxidized by oxygen of the feed gases.

One of the problems is to overcome the activation energy necessary for initial hydrogen abstraction from the highly resonance-stabilized α-methylstyrene system. Also it is imperative to have a catalyst with isolated sites (14) (i.e., isolated active oxygen domains) to prevent the complete combustion of α-methylstyrene or the formation of thermodynamically very stable benzonitrile.

The catalytic site cannot be too acidic for two reasons. The first is to prevent the attack of α-methylstyrene at the double bond and thus the immediate loss of the methylene group. The second is to prevent the formation of a strong chemisorbed reaction intermediate–catalyst complex, which would be difficult to desorb as atroponitrile; at best benzonitrile would be formed from such a system.

These requirements call for a catalyst with isolated, easily exchangeable, active oxygens, possessing only mild acidity. From our fundamental work on the surface reaction chemistry of Sb-based catalysts (15, 16) and the ammoxidation reaction mechanism of propylene over heterogeneous catalysts (17), we conclude that an existing catalyst fitting the requirements is the U–Sb–O system or one of its modifications. Group VIII modified U–Sb-oxides, Bi- and/or Mo-modified Fe–Sb-oxides, Sn–Sb–oxides, and Sn–Pb–molybdates are some other catalysts which our theory predicts would be useful for the reaction. Catalysts such as Bi–phosphomo-

lybdate, V_2O_5, and vandates are predicted by this reasoning to be much less useful in the ammoxidation of α-methylstyrene to atroponitrile than are antimony oxide-based systems.

<div style="text-align:center">EXPERIMENTAL</div>

α-Methylstyrene (αMS), β-methylstyrene (a 15 : 85 cis : trans mixture), and allylbenzene were obtained commercially and used without further purification. $USb_{4.6}O_{13.2}$ catalysts were prepared by the method of Grasselli and Callahan described below (18).

Catalyst Preparation

Method A. A high-surface-area (42 m²/g) catalyst of composition $USb_{4.6}O_{13.2}$ (70 wt%) · SiO_2 (30 wt%) was prepared by addition of $UO_2(NO_3)_2 \cdot 6H_2O$ (81.4 g) to a solution of Sb metal (90 g) in 360 ml hot, concentrated HNO_3 and the mixture refluxed until brown fumes of NO_x ceased to evolve (~45 min). After cooling, duPont Ludox AS (30 wt% SiO_2 sol, 228.4 g) was added to the slurry, followed by pH adjustment to 8.0 with 28% NH_4OH. The resulting slurry was filtered, dried at 120°C for 8 hr, heated at 430°C for 3 hr to decompose nitrates, calcined at 980°C for 8 hr and ground and screened to 20–35 mesh size. (Catalyst USb-42.)

Method B. Catalysts of composition $USb_{4.6}O_{13.2}$ (60 wt%) · SiO_2 (40 wt%) were prepared by refluxing Sb_2O_3 (322.8 g) and U_3O_8 (grade I, 136.2 g) in 800 ml concd HNO_3 for 45 min until NO_x evolution ceased. After cooling, 655.7 g duPont Ludox AS (30 wt% SiO_2 sol) was added to the slurry and pH adjusted to 8.0 with 28% NH_4OH. The solid was filtered and washed with 3 × 300 ml water, dried for 1 hr at 225°C (initial drying), decomposed at 430°C for 3 hr and heat-treated at 940°C for 8 hr. The resulting catalyst (665 g) was mixed with 347 g Ludox (30 wt% SiO_2 sol) in a blender, extruded, dried overnight at 120°C (final drying), and calcined at 940°C for 71 hr (final calcination). The resulting material

had a surface area of 29 m²/g (Catalyst USb-29).

Using Method B with an initial drying at 120°C for 12 hr and decomposition at 430°C for 24 hr produced a catalyst of 15 m²/g surface area (Catalyst USb-15).

Using this same procedure (method B), except with an initial drying at 120°C for 12 hr, decomposition at 430°C for 24 hr, and a final calcination at 1000°C for 6 hr, produced a catalyst of surface area 7 m²/g (Catalyst USb-7).

Promoted catalysts. These were prepared using Method A with addition of 1% promoter elements as Nb_2O_5, $Th(NO_3)_4$, or Ta_2O_5 to the filtered and washed precipitate resulting from adjustment to pH 8.

Apparatus and procedures. A 5-cm³ microreactor was used for all runs. Results and experimental conditions are shown in Figs. 1–7 and Table 1 for α-methylstyrene and Table 4 for β-methylstyrene and allylbenzenes. Gas/liquid chromatographic results were obtained using a 2-meter 20% DC 200 (200 cSt) on Celite W column. Recovery runs were performed by collecting the effluent from the heated exit line in an absorber consisting of a gas dispersion tube immersed in a mixture of n-propanol/H_2O/HCl (90:9:1) and a glass wool trap. In n-propanol solution, the monomer is quite stable and can be stored for months at 0°C without any apparent changes. While a 14% (wt) solution of atroponitrile in benzene has a half-life of 103 hr at room temperature, even pure atroponitrile can be stored indefinitely at −78°C. The dimerization reaction is discussed in more detail under Results and Discussion.

Spectroscopic analyses. For ir analysis, the effluent was trapped in KBr powder, which was placed into a 6-mm × 3-cm glass tube attached directly to the exit line of the chromatograph; the spectra consisted of the following bands (cm⁻¹): 3110 (w, =CH₂), 3087 (w, =CH₂), 3064 (m, =CH₂), 3033 (m, Ar—H), 2270 (w, broad), 2233 (m, —CN), 1950 (w, br), 1880 (w, br, C=CH₂),
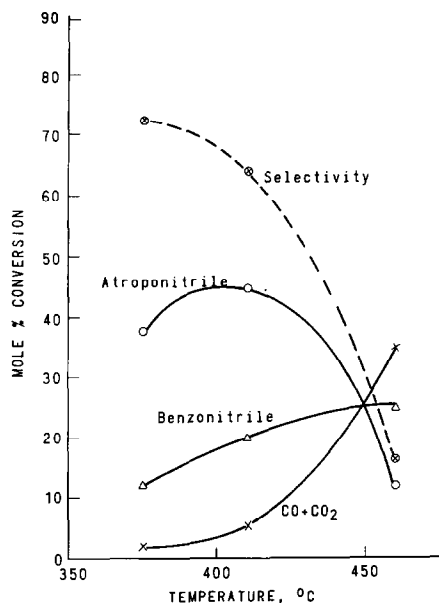

FIG. 1. Effect of temperature in ammoxidation of α-methylstyrene, high-surface-area $USb_{4.6}O_{13.2}$ (70%) · SiO_2 (30%). Surface area = 42 m²/g; contact time = 0.5 sec; α-Me–styrene/NH₃/Air/N₂ = 1/1.5/50/72.5; Catalyst USb-42, 5 cm³.
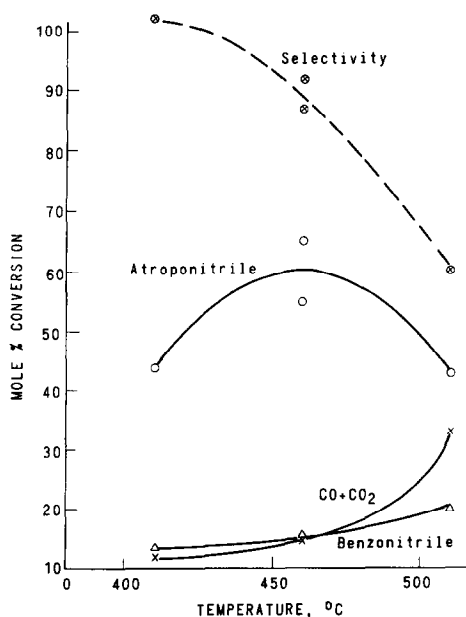

FIG. 2. Effect of temperature in ammoxidation of α-methylstyrene, low-surface-area $USb_{4.6}O_{13.2}$ (70%) · SiO_2 (30%). Surface area = 7 m²/g; contact time = 0.5 sec, 0.4 sec (410°C); α-Me–styrene/NH₃/Air/N₂ = 1/1.5/50/72.5; Catalyst USb-7, 5 cm³, 4 cm³ (410°C).
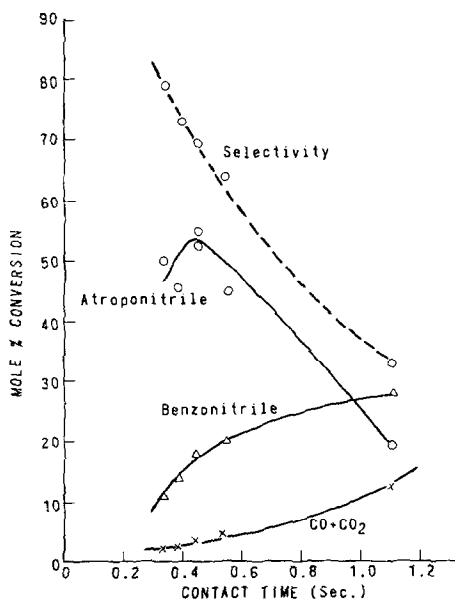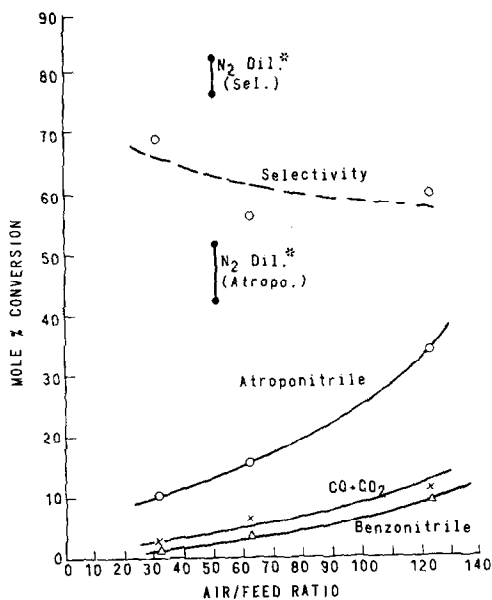
FIG. 3. Effect of contact time on ammoxidation of α-methylstyrene at 410°C, high-surface-area USb$_{4.6}$O$_{13.2}$ (70%) · SiO$_2$ (30%). Surface area = 42 m²/g; temperature = 410°C; α-Me–styrene/NH$_3$/Air/N$_2$ = 1/1.5/50/72.5; Catalyst USb-42, 3–5 cm³.

*Feed/air/N$_2$ = 1/50/72.5

FIG. 5. Effect of air/α-MS ratio in Ammoxidation of α-methylstyrene at 460°C, low-surface-area USb$_{4.6}$O$_{13.2}$ (70%) · SiO$_2$ (30%). Surface area = 7 m²/g; temperature = 460°C; contact time = 0.5 sec; αMS/NH$_3$/Air/N$_2$ = 1/1.5/31–123/0; Catalyst USb-7, 5 cm³.
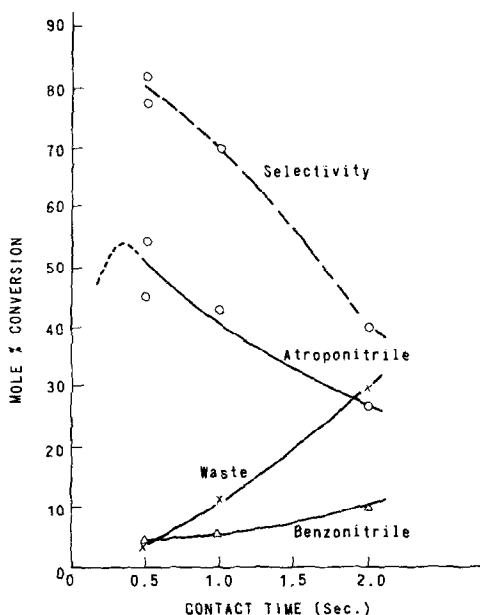
FIG. 4. Effect of contact time on ammoxidation of α-methylstyrene at 460°C, low-surface-area USb$_{4.6}$O$_{13.2}$ (70%) · SiO$_2$ (30%). Surface area = 7 m²/g; temperature = 460°C; α-Me–styrene/NH$_3$/Air/N$_2$ = 1/1.5/50/72.5; Catalyst USb-7, 5 cm³.
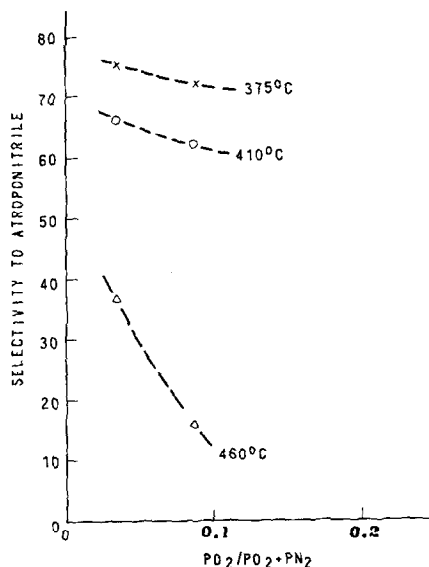
FIG. 6. Effect of P_{O_2} in ammoxidation of α-methylstyrene, high-surface-area USb$_{4.6}$O$_{13.2}$ (70%) · SiO$_2$ (30%). Surface area = 42 m²/g; contact time = 0.5 sec; Catalyst USb-42, 5 cm³; αMS/NH$_3$ = 1/1.5; α-MS/total = 1/12.5.
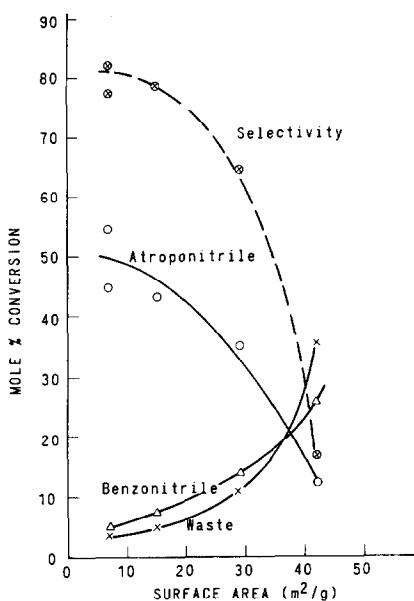
FIG. 7. Effect of $USb_{4.6}O_{13.2} \cdot SiO_2$ catalyst surface area in ammoxidation of α-methylstyrene at 460°C. Temperature = 460°C; contact time = 0.5 sec; α-Me-styrene/NH_3/Air/N_2 = 1/1.5/50/72; Catalysts USb 42, 29, 15, 7; 5 cm³ each.

1740 (w, br), 1680 (w, br), 1607 (m, C=C olefinic + aromatic), 1570 (m), 1495 (m, C=C aromatic), 1450 (m, C—C skeletal), 1400 (w, br), 1290 (w, br), 1270 (m), 1180 (w, br), 1150 (w, br), 1070 (w), 1025 (m), 930 (s, br, C=CH$_2$), 895 (w), 840 (w, br), and 773 (s), 717 (s), 684 (s) (monosubstituted aromatic C—H).

NMR samples were prepared by collecting the portion of the effluent containing atroponitrile which gave the following spectrum (C_6D_6, ppm downfield from TMS): 5.40 (s), 5.55 (s) (methylene protons), and 6.60–7.73 (br, m, aromatic).

A low-voltage mass spectral analysis of the atroponitrile monomer used for NMR and ir analyses showed an M^+ peak at 129 m/e as expected, but no 258 (dimer).

RESULTS AND DISCUSSION

1. Ammoxidation of α-Methylstyrene to Atroponitrile

—(a) $USb_{4.6}O_{13.2}$ catalyst. $USb_{4.6}O_{13.2}$ was found to be an active and selective catalyst for ammoxidation of α-methylstyrene (αMS), consistent with our theory (15, 16) concerning the properties required for a good catalyst in this reaction. For this reason, we have investigated process variables over a wide range of conditions for this catalyst. Contact time, feed-to-air-and-diluent ratio, catalyst surface area, temperature of reaction, and oxygen partial pressure were the main variables investigated. The pertinent data of this study, performed in 5-cm³ microreactor units, are described under Experimental.

(b) Reaction temperature. The effect of temperature on conversion and selectivity to atroponitrile is shown in Fig. 1 with a catalyst of 42 m²/g surface area (USb-42). The maximum conversion to atroponitrile lies at about 410°C. The selectivity is highest at still lower temperatures. At 350°C, almost no reaction took place, while at 500°C, the reaction was too severe, yielding mainly CO_2 and water.

For the catalyst of 7 m²/g (USb-7, Fig. 2) the maximum conversion to atroponitrile lies somewhere around 460°C. The general profile of conversion and selectivity versus temperature is similar to that found for USb-42, with the atroponitrile yield maximum shifted to higher temperature. In addition to this shift, the atroponitrile selectivities are considerably better with the low-surface-area catalyst at comparable conversion levels. It is very likely that a catalyst with still lower surface area would yield even better atroponitrile conversion, be even more specific, and could also be operated at still higher temperatures.

(c) Contact time. There is a strong effect of contact time on selectivity and conversion to atroponitrile, both of which are optimized at short contact times (Figs. 3 and 4).

(d) Effect of air : αMS ratio. Converison to atroponitrile dropped off rapidly, while selectivity remained about the same when the air/αMS ratio was lowered from 120 : 1 to 30 : 1 (Fig. 5). In addition, the activity of the catalyst decreased more rapidly at the

TABLE 1

Ammoxidation of α-Methylstyrene Using Promoted $USb_{4.6}O_{13.2}$ (70%) · SiO_2 (30%) (USb-42)

Promoter		Weight percent promoter	Unconverted α-methylstyrene (αMS)	Percentage yields				Material balance (Σ Prod. + αMS)	Percentage reacted (Σ prod.)	Percentage selectivity to atroponitrile
				Atropo-nitrile	Benzo-nitrile	CO_2	CO			
410°C 4-cm³ catalyst, 0.44 sec contact time	Nb	1.04	11.0	57.4	9.3	1.4	—	79.1	68.1	84
	Unpromoted		6.4	55.1	17.7	3.4	—	82.6	76.2	72
	Th	2.54	36.7	46.8	5.8	—	—	89.3	52.6	89
	Ta	1.11	28.4	43.1	5.2	0.7	—	77.4	49.0	88
46C°C 5-cm³ catalyst, 0.51 sec contact time	Th	2.54	—	40.4	15.7	19.1	—	75.2	75.2	54
	Unpromoted		0	11.9	25.4	29.0	6.1	72.4	72.4	16

Note. Catalyst particle size = 20–35 mesh; α-Me–Styrene/NH_3/Air/N_2 = 1/1.5/50/72.5.

TABLE 2

X-Ray Diffraction Spectrum of Crystalline
Atroponitrile Dimer

d (Å)	Percentage I/I_1	d (Å)	Percentage I/I_1
8.378	57.7	2.901	2.3
6.553	32.0	2.846	1.3
6.366	22.4	2.769	10.6
5.587	71.2	2.736	2.6
5.417	17.3	2.728	2.8
5.181	41.7	2.680	5.9
5.049	6.4	2.650	1.4
4.870	7.7	2.627	1.8
4.704	10.3	2.612	2.5
4.514	100.0	2.576	6.2
4.480	60.9	2.569	3.5
4.019	35.9	2.499	1.6
3.931	2.9	2.415	3.8
3.798	28.8	2.396	6.4
3.767	31.4	2.366	4.6
3.743	38.5	2.342	1.9
3.675	29.8	2.319	1.0
3.616	5.3	2.252	1.8
3.608	8.5	2.231	1.8
3.524	22.4	2.199	2.4
3.490	4.5	2.189	2.3
3.424	7.1	2.184	2.0
3.411	7.3	2.149	4.3
3.288	21.8	2.144	4.1
3.252	16.4	2.120	2.7
3.229	4.0	2.101	2.6
3.189	4.1	2.026	1.9
3.178	5.8	2.017	1.9
3.151	10.1	2.009	2.5
3.051	9.9	2.004	2.7
3.046	9.3	1.996	2.6
2.986	12.8	1.992	2.4
2.938	3.4	1.861	2.5
2.919	2.6		

low air-to-αMS ratio than at higher ones. This suggests two explanations. One is that simply not enough oxygen is supplied to the catalyst to keep it oxidized. The other is that atroponitrile does not get desorbed effectively from the surface at higher αMS partial pressures. Since high conversions are obtained at relatively low partial pressures of oxygen, provided that the air + diluent-to-feed ratio is kept high, the latter is a more likely explanation. In fact, the best results are obtained with nitrogen dilution (feed/air/N_2 = 1/50/72.5).

(e) *Effect of P_{O_2}* (42 m²/g catalyst, Fig. 6). At high oxygen partial pressure, selectivity suffers. This is particularly noticeable at high reaction temperatures. It points to a possible afterburn problem, or, since the surface area of the catalyst tested was relatively high, to excessive catalyst activity.

The effect of high oxygen partial pressure on selectivity was less pronounced at lower temperatures. However, it is difficult to maintain U/Sb catalysts in a high oxidation state at 375°C and below. Therefore, a catalyst surface area study was undertaken aimed at bringing the surface area of catalysts down so that they could then operate at a higher temperature.

(f) *Surface area.* As shown in Fig. 7, the effect of surface area is quite pronounced. At practical operating temperatures of 460°C, the lower-surface-area catalysts behave more favorably. With USb-7, conversions of 45 to 55% to atroponitrile were obtained with selectivities of 80%.

(g) *Promoted $USb_{4.6}O_{13.2}$*. At 410°C, the atroponitrile selectivities of several promoted catalysts are markedly better than those of the base catalyst (Table 1). The per pass conversions are comparable to the base catalyst. At 460°C, the selectivity difference between the promoted and base catalysts is even more pronounced. It is apparent that addition of selected promoters is an alternative to reducing surface area of the base catalyst in achieving good selectivity at higher operating temperatures (460°C).

Particularly noteworthy are the Group VA elements (Nb, Ta) and Th. Niobium and tantalum are known to form compounds with uranium which belong to a similar crystallographic class as the active phase of the $USb_{4.6}O_{13.2}$ catalyst (16). Therefore, they can easily enter Sb lattice positions substitutionally. The behavior of Th and U is, of course, very similar.

The improvements achieved by Nb, Ta, and Th promotion are primarily due to a separation of active site domains of the

base U–Sb–oxide system resulting in increased selectivity. This occurs on the surface, as well as in the bulk, owing to substitution of Sb positions. This reasoning is consistent with the postulates presented earlier by Grasselli and co-workers (*14, 16, 21*). The improvement in performance realized by the addition of Group VIII elements is primarily due to better electron transfer and improved oxygen mobility of the base catalyst. This is also consistent with our earlier postulates (*14, 16, 21*).

Small amounts of alkaline earths may be beneficial for enhanced selectivity, although they do lower the activity somewhat. Acidic promoters have a deleterious effect.

The best overall results were obtained with a 1% Nb-promoted catalyst which gave a conversion to atroponitrile of 57% per pass with a selectivity of 85%.

(*h*) *Effect of NH$_3$: α-methylstyrene ratio.* Ratios in excess of 1.5 : 1 are not desirable. Excess ammonia suppresses the desired reaction and the feed passes essentially unreacted through the reactor. The stoichiometric requirement of 1 : 1 or a slightly higher ratio is sufficient.

(*i*) *Unsupported catalyst.* The unsupported catalyst was very active and unselective, yielding virtually only CO_2 and water, plus some benzonitrile under the conditions tested.

2. Oxidation of α-Methylstyrene to Atropoaldehyde

The direct catalytic conversion of α-methylstyrene to atropoaldehyde was also investigated. A large number of catalytic compositions was tested. As for ammoxidation, the best results were obtained at 410°C with a Nb-promoted $USb_{4.6}O_{13.2}$ catalyst which yielded 30% per pass atropoaldehyde with a selectivity of 60%. The aldehyde may prove to be a valuable monomer and/or chemical in its own right (*18, 19*).

3. Dimerization of Atroponitrile

Upon prolonged standing, white crystals precipitated from a 10% solution of atroponitrile. A batch of these crystals was purified by recrystallization from acetic acid/methanol, and had the following properties:

(a) *mp* 121–123°C (lit. (*5*) 123–124°C).

(b) *ir* (*KBr, crystalline form*): 3070 (w), 3010 (m), 2940 (m), 2880 (w), 2240 (m), 1980 (w), 1950 (w), 1870 (w), 1595 (w), 1580 (w), 1480 (s), 1445 (s), 1400 (w), 1360 (w), 1330 (w), 1290 (w), 1260 (w), 1090 (w), 1070 (w), 1040 (w), 1020 (w), 990 (m), 955 (w), 910 (w), 840 (w), 765 (s), 755 (s), 700 (s), 660 (w), 640 (w), 620 (m), 595 (w), 550 (m), 520 (w), 500 (m), 480 (w), 450 (w), 410 (w).

(c) *ir* (*melt, amorphous form*): 3060 (m), 3030 (w), 2960 (w), 2940 (w), 2880 (w), 2270 (w), 2240 (m), 1950 (w, br), 1870 (w), 1805 (w, br), 1770 (w), 1730 (w), 1670 (w), 1595 (m), 1580 (w), 1490 (s), 1445 (s), 1420 (w), 1330 (w), 1280 (w, br), 1220 (w), 1190 (w), 1150 (w), 1070 (w), 1030 (m), 1020 (m), 1000 (m), 980 (m), 975 (m), 920 (w), 900 (w), 830 (w, br), 780 (m), 755 (s), 695 (s), 655 (w), 630 (m), 600 (w), 570 (m).

(d) *NMR* ($CDCl_3$): 2.00–2.60 (m, 4H), 4.10 (t, 1H, J = 5.0 Hz), 7.00–7.46 (m, 9H).

(e) *XRD* of the crystalline form is shown in Table 4; that of the amorphous form

TABLE 3

Kinetics of Atroponitrile Dimerization in Benzene Solution

Temp. (°C)	k^a (liter-mole^{-1}-sec^{-1})	$t_{\frac{1}{2}}^a$ (hr)
58	6.76×10^{-5}	7.0^b
23	4.87×10^{-6}	98^b
9.5	1.40×10^{-6}	338^b
0	5.37×10^{-7}	885^c
−78	9.99×10^{-12}	4.77×10^{7c}

^{a} Initial concentration = 0.55 M (14 wt%).
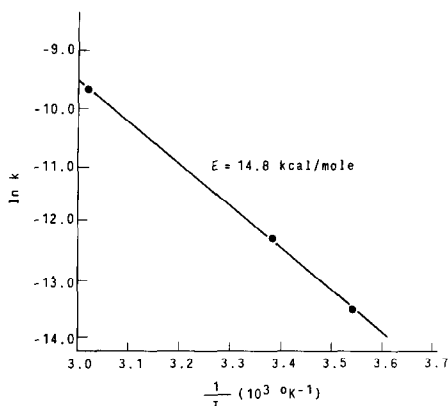^{b} Points determined experimentally.
^{c} Calculated values.

FIG. 8. E_a of dimerization of atroponitrile in benzene solution.

showed two very broad overlapping bands of about equal intensity centered at d values of 6.804 and 4.227 Å.

(f) *DTA*. All analyses were performed at a heating rate of 5°C/min, unless otherwise specified. The crystalline form of the DPT exhibits only one endotherm at its melting point, 122°C. On cooling, no thermal activity was detected. Analysis of the melt by infrared showed it to be identical to the amorphous form, which exhibits an exotherm at 81°C, and endotherms at 103 and 120°C, with no thermal activity on cooling. When the amorphous form was heated at

2.5°C/min, an exotherm at 78.4°C and one broad endotherm at 120.6°C were observed.

Rate of dimerization. The kinetics of dimerization were determined by following the loss of atroponitrile monomer from 10–20% (wt) benzene solutions using vapor-phase chromatography. Second-order rate constants were determined at 9.5, 23, and 58°C (Table 3), and the corresponding Arrhenius plot (Fig. 8) gives an E_a of 14.8 kcal/mole, consistent with previous studies (22). Free radical inhibitors such as indigo carmine or methylene blue had no significant effect on the reaction rate.

Our evidence which confirms the structure as DPT, supports that of Newey and Erickson (5), but is not consistent with the cyclobutane structure 4 proposed by Walker (8). The second order kinetics, low E_a (14.8 kcal/mole), and the insensitivity of reaction rate to the presence of free radical and oxidation inhibitors in the dimerization of atroponitrile to DPT is indicative of a rate-determining Diels–Alder reaction followed by a fast aromatization (formal 1,3-hydrogen shift) resulting in both diasteriomeric forms of DPT, as depicted below (Eq. (3)).

(3)
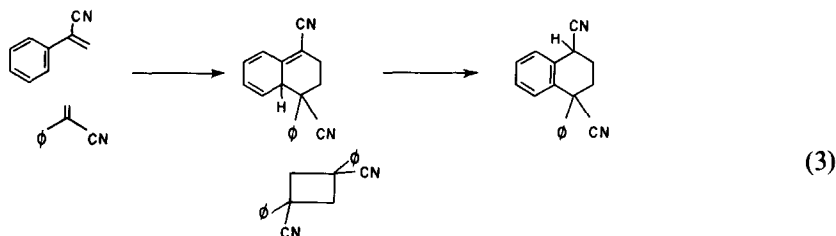
Crystalline–amorphous interconversion of DPT. The atroponitrile dimer DPT exists in both a crystalline and an amorphous form. The crystalline dimer melts at 121–123°C, but once melted, it converts to an

amorphous state. Conversion back to the original crystalline state can be accomplished by simple physical grinding or agitation, or by bringing a crystal of the dimer into intimate contact with the amorphous

TABLE 4

Ammoxidation of Allylbenzene and β-Methylstyrene at 460°C on 60% $USb_{4.6}O_{13.2}$–40% SiO_2 (Sb-7)[a]

Olefin	Percentage yields						Material balance (Σ prod. + olefin)	Percentage reacted (Σ prod.)	Percentage selectivity to Cinnamo-nitrile
	Olefin	Cinnamo-nitrile	Benzo-nitrile	CO_2	CO	[b]			
Allylbenzene	1.7	57.8	4.6	1.7	—	7.8	65.8	64.1	80
β-Methylstyrene	32.0	20.1	15.9	3.7	1.9	6.0	73.6	41.6	42

[a] Method B, 7 m^2/g.
[b] Unidentified products.

phase. The ir spectra of the two forms are very different as are the XRD spectra, in which the sharp, intense lines of the crystalline state (Table 2) are converted to two very broad lines after transformation to the amorphous state by melting. The NMR spectra and the molecular weight of the two forms are identical, which eliminates the formation of polymer in the transformation. From DTA experiments no lower melting form could be detected, as would be expected if the presence of a metastable form resulted in monotropic polymorphism. An exotherm at 81°C for the amorphous state, not present in the crystalline DTA, is probably the result of a solid-state structural reordering.

4. Ammoxidation of Allylbenzene and β-Methylstyrene to Cinnamonitrile

Both allylbenzene and β-methylstyrene can also be ammoxidized using $USb_{4.6}O_{13.2}$ to give cinnamonitrile as the selective product, with 80 and 42% selectivi-ties, respectively (Table 4). However, the rate of formation of cinnamonitrile from allylbenzene is 2.9 times faster than from β-methylstyrene. This strongly suggests that both reactions proceed via a common allylic intermediate, which is formed faster from the allylbenzene, the less-stable olefinic isomer.

CONCLUSIONS

The direct ammoxidation of α-methylstyrene to atroponitrile has been accomplished with conversion of 55% per pass and selectivity of 80% to atroponitrile at 460°C, under special reaction conditions, using a U–Sb–oxide catalyst. This process is similar in nature to the ammoxidation of propylene to acrylonitrile and isobutylene to methacrylonitrile (MAN), in which an allylic intermediate is formed by H abstraction in the initial rate-determining step, followed by =NH insertion, further oxidation, and desorption of the unsaturated nitrile (17), as depicted below (Eq. (4)).

$$ \text{(4)} $$

R = H, AN process
R = φ, atropo process
R = Me, MAN process
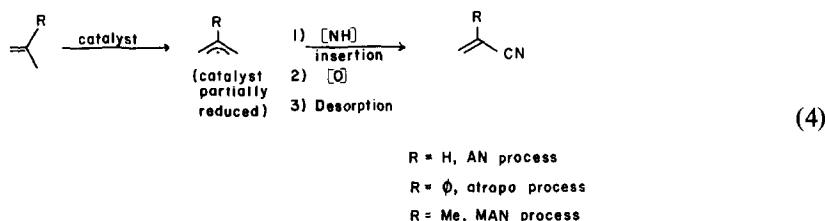
However, this process requires short contact times (0.5 vs 3.4 sec for MAN process), a low-surface-area catalyst (7 vs 42 m^2/g for MAN process), and dilution of

feed with N_2 or some other inert diluent for optimal results. It is necessary to quickly remove the highly reactive atroponitrile from the reactor to minimize dimerization, polymerization, and condensation reactions.

The addition of Group VA promoters, especially Nb, is an alternative to lowering surface area to increase selectivity. These promoters form structures with U which stabilize the active phase of the catalyst and separate active site domains from each other. Group VIII elements added as promoters enhance the electron and lattice oxygen transport properties of the base catalyst system. The end result of such selected promoter additions is enhanced selectivity and/or activity of the resulting catalyst at comparable or similar reaction conditions.

Optimal reaction conditions call for intermediate partial pressures of oxygen: high enough to sustain the catalyst surface in a favorably high oxidation state, yet low enough to prevent excessive combustion of the atroponitrile.

In a direct catalytic oxidation process, similar to the ammoxidation process but with no ammonia in the feed stream, α-methylstyrene can be converted to atropoaldehyde in good yields (e.g., 30% per pass conversion, 60% selectivity) with a Nb-promoted U–Sb–oxide catalyst.

A comparison of the aromatic nitrile formation rates from α-methylstyrene, β-methylstyrene, and allylbenzene, suggests that the ammoxidation of aromatic olefins proceeds through a common allylic intermediate.

REFERENCES

1. Frank, E. K., U.S. Patent 3,063,961, November 13, 1962.
2. Hardwicke, N. L., U.S. Patent 2,947,738, August 2, 1960; Kreisel, M., Garbatski, U., and Kohn, D. H., *J. Polymer Sci.* Part A, **2**, 105 (1964).
3. Regeaud, J.-P., *Chim. Mod.* **4**, 91 (1959); Perry, E., U.S. Patent 3,322,742, May 30, 1967; Hoefelmann, K., Sattelmeyer, R., and Hamann, K., *Makromol. Chem.* **112**, 2 (1968); Hughes, L. J., and Perry, E., *J. Polymer Sci.*, Part A, **3**, 1527 (1965).
4. Cologne, J., Dreaux, J., and Regeaud, J.-P., *Compt. Rend.* **246**, 438 (1958).
5. Newey, H. A., and Erickson, J. G., *J. Amer. Chem. Soc.* **72**, 5645 (1950), and references cited therein.
6. Stewart, J. M., and Chang, C. H., *J. Org. Chem.* **21**, 635 (1956).
7. Vigier, A., and Dreaux, J., *Compt. Rend.* **252**, 3598 (1961).
8. Walker, J. F., U.S. Patent 2,478,990, August 16, 1949; Sackmann, G., and Funke, W., *Makromol. Chem.* **123**, 4 (1969).
9. Cologne, J., Dreaux, J., and Regeaud, J.-P., *Bull. Soc. Chim. Fr.* 1244 (1959).
10. Funke, W., *Angew Chem.* **72**, 750 (1960).
11. Clifford, A. M., and Long, J. R., U.S. Patent 2,362,049, November 7, 1944.
12. Grasselli, R. K., and Miller, R. C., U.S. Patent 3,686,295, August 22, 1972.
13. Mekhtiev, S. D., Rizaev, R. G., Novruzova, A. Sh., Akhmedov, S. M., and Rafiev, M. S., USSR Patent 253,798, March 21, 1972.
14. Callahan, J. L., and Grasselli, R. K., *AIChE J.* **9**, 755 (1963).
15. Grasselli, R. K., and Callahan, J. L., *J. Catal.* **14**, 93 (1969); for additional structural work, see Grasselli, R. K., Suresh, D. D., and Knox, K., *J. Catal.* **18**, 356 (1970).
16. Grasselli, R. K., and Suresh, D. D., *J. Catal.* **25**, 273 (1972).
17. Burrington, J. D., and Grasselli, R. K., *J. Catal.* **59**, 79 (1979); Burrington, J. D., Kartisek, C. T., and Grasselli, R. K., *J. Catal.* **63**, 235 (1980).
18. Grasselli, R. K., and Callahan, J. L., U.S. Patent 3,435,061, March 25, 1969; Grasselli, R. K., U.S. Patent 3,452,032, June 24, 1969 (Re 27,171).
19. Grasselli, R. K., U.S. Patent 3,325,504, June 13, 1967.
20. Grasselli, R. K., and Callahan, J. L., U.S. Patent 3,546,174, December 8, 1970; U.S. Patent 3,501,470, March 17, 1970.
21. Callahan, J. L., Grasselli, R. K., Milberger, E. C., and Strecker, H. A., *Ind. Eng. Chem. Prod. Res. Develop.* **9**, 134 (1970).
22. Hopff, H., Lüssi, H., and Borla, A., *Helv. Chim. Acta* **46**, 723 (1963).